Cume #340 (*with solutions*)
(5 Questions; 85 Points Possible; 70 Points Guaranteed Pass)
Given January 24, 2009

Partial Coverage and Time Variability of Narrow–Line Intrinsic QSO Absorption Systems
Barlow, T. A., Hamman, F., & Sargent, W. L. W., in "Mass Ejection From AGN,"
eds. R. Weymann, I. Shlosman, & N. Arav (arXiv:astro-ph/9705048v1)

Please start each question (by number) on a new sheet of paper, write on only one side of the paper, and staple them together in order of question number when finished.

1. **[13 pts]** Intrinsic and Intervening Absorption

(a) [5 pts] Define what an intervening absorber is. List as many properties as you can of what characterizes an intervening QSO absorption line system.

Intervening absorbers are absorbing gas structures that are not physically associated with the QSO environment nor with the quasar host galaxy nor with the cluster in which the quasar host galaxy resides. In the abstract, the authors state that intervening absorbers are "gas clouds unrelated to the QSO phenomenon". Intervening absorbers are at cosmological distances from the background QSO and their redshift separations from the QSO are due to the Hubble flow. Intervening absorbers are often associated with intergalactic gas such as Lyα *forest clouds, intracluster or intragroup gas, or galactic disk or halo gas. The velocity widths range between 20 to 400 km* s^{-1} *and the absorption profiles exhibit velocity splittings due to the kinematics of multiple distinct clouds at different line of sight velocities. Also, the gas is usually photoionized by the ultraviolet background radiation.*

(b) [5 pts] Define what an intrinsic absorber is. List as many properties as you can of what characterizes an intrinsic QSO absorption line system.

Intrinsic absorbers are physically associated with the QSO central engine (cute talk for the region that generates the quasar continuum). In the abstract, the authors state that intrinsic absorbers are "gas clouds within the QSO environment". Physically, intrinsic absorbers are winds, ejecta, or infalling material local to the QSO. Intrinsic absorbers are influenced by the QSO radiation field, and partake in the dynamical interaction of the QSO with its environment. The velocity spreads of the absorption profiles are often larger than those of intervening absorbers, > 600 *km* s^{-1}*, and the profiles exhibit the characteristic shapes of winds or smooth gas flows, as opposed to discrete clouds. In the first paragraph of § 2 of the paper, the authors outline nine (9) properties that distinguish an absorber as an intrinsic absorber. It was not necessary to write down all these properties. One important property is that the redshift of the absorption is very close to the redshift of the QSO. The velocity relative to the QSO is usually within some 50,000 km* s^{-1}*, and in extreme cases, the velocity widths of the absorption lines can be 5000 km* s^{-1}*. Some properties that are important are (1) time variability, (2) saturated profiles, (3) partial covering, (4) very high metallicity, and (5) high electron densities.*

(c) [3 pts] Describe the third type of system, that does not strictly follow the definition of either an intervening absorber nor an intrinsic absorber?

Somewhere between the intervening absorbers and the intrinsic absorbers are those that physically reside in the QSO host galaxy or the galaxy cluster hosting the QSO. Some researchers call these "associated" absorbers. Associated absorbers are not winds, ejecta, or infalling to the QSOs themselves. The redshift of these absorbers are close to the redshift of the QSO. The properties of these absorbers are similar to the intervening absorbers, except that the probability of intercepting them is higher than for intercepting the intervening absorbers.

2. **[7 pts]** Given the emission redshift and absorption redshift of the Q0449–13 system discussed in the beginning of § 3 and illustrated in Figure 1 of the paper, show by means of calculation that the outflow velocity is the stated 3000 km s^{-1}.

Since the velocity difference (or outflow velocity) is non relativistic, the quick and dirty answer is

$$\frac{\Delta v}{c} = \frac{z_{\rm abs} - z_{\rm em}}{1 + z_{\rm em}},$$

where $z_{\rm abs}$ *is the absorber redshift and* $z_{\rm em}$ *is the emission redshift of the QSO. We have*

$$\Delta v = c \left[\frac{3.053 - 3.094}{1 + 3.094} \right] = -0.01c = -3000 \text{ km s}^{-1},$$

This result can be obtained several ways. The first is that $v = cz$ *for non relativistic velocities. We can apply this equation because we are computing the velocity difference in the inertial frame of the QSO. So* $\Delta v = cz_{\rm abs} - cz_{\rm em}$. *But this is the co–moving velocity difference. To obtain the proper velocity, divide by* $1 + z_{\rm em}$. *The expression for* Δv *can also be obtained directly from the non–relativistic Doppler formula,* $\Delta v/c = \Delta\lambda/\lambda$. *If* $\lambda_o = \lambda_r(1+z)$ *is the observed wavelength and* λ_r *is the rest–frame wavelength for an emitter or absorber at redshift* z, *then*

$$\frac{\Delta v}{c} = \frac{\Delta\lambda}{\lambda} = \frac{\lambda_r(1 + z_{\rm abs}) - \lambda_r(1 + z_{\rm em})}{\lambda_r(1 + z_{\rm em})} = \frac{(1 + z_{\rm abs}) - (1 + z_{\rm em})}{1 + z_{\rm em}} = \frac{z_{\rm abs} - z_{\rm em}}{1 + z_{\rm em}}.$$

Relaxing $\Delta v \ll c$, *we are required to employ the well known relativistic Doppler formula to obtain the peculiar velocity,*

$$1 + \frac{z_{\rm abs} - z_{\rm em}}{1 + z_{\rm em}} = \sqrt{\frac{1 + \Delta v/c}{1 - \Delta v/c}},$$

where the factor $1 + z_{\rm em}$ *ensures that* Δv *is the inertial frame peculiar velocity (omitting this factor provides the co–moving peculiar velocity). Inverting, we have*

$$\frac{\Delta v}{c} = \frac{\left[1 + \dfrac{z_{\rm abs} - z_{\rm em}}{1 + z}\right]^2 - 1}{\left[1 + \dfrac{z_{\rm abs} - z_{\rm em}}{1 + z}\right]^2 + 1},$$

which reduces to the non–relativistic case for $(z_{\rm abs} - z_{\rm em})/(1 + z_{\rm em}) \ll 1$.

Many of you applied the relativistic Doppler formula to compute the recessional velocity of the absorber and then of the QSO, and then took the difference to obtain the velocity separation. This is wrong on multiple levels. First, the relativistic Doppler formula does NOT yield the cosmological recessional velocity. Second, the formula was applied to obtain the recessional velocity in the observer frame; but it can only be applied this way if the receding object is in the inertial frame of the observer, which is NOT true for cosmological objects.

*[*** This is important stuff. I have attached a couple of pages from my book to this solution set that you are welcome to read if you want to better understand and learn how to compute velocities and velocity differences in the cosmological setting. ***]*

3. **[25 pts]** The authors state that time variability is probably the most conclusive indicator that an absorber is intrinsic.

(a) [6 pts] Identify and qualitatively describe the two physical processes mentioned by the authors that potentially yield variability in the absorption lines of an intrinsic absorber?

(1) The luminosity and/or spectral energy distribution of the ionizing source (QSO) can vary, which results in a changed flux at the absorbing cloud. This changed flux can result in a change in the ionization conditions of the absorbing cloud. (2) If the absorbing cloud is moving at a substantial velocity relative to source, this can potentially be observed. Since the shape of the absorption line maps the velocity distribution of the optical depth, this distribution can change over time. Both of these physical processes can potentially be observed even when partial covering is present. In fact, #2 may be enhanced by a change in the partial covering with time.

(b) [19 pts] The authors mention that it is possible to distinguish between these two physical mechanisms "by observing two different lines of different ionization levels". Let's call the two physical mechanisms, Mech1 and Mech2 (so as to not have me give away what they are in the question). Now, say you needed to perform this experiment. Describe very precisely how you would undertake the experiment, including (i) on what basis would you choose which lines to study? (ii) what quantity or quantities would you measure for each of these lines in order to quantitatively compare them? (iii) how would you expect this quantity to vary if the variability were due to Mech1? or (iv) how would you expect this quantity to vary if the variability were due to Mech2? [Basically, I am asking you to design and very clearly describe the experiment and clearly state your hypothesis]

If the hypothesis is that the source luminosity is variable, then one should examine changes in the ionization conditions. A sure experiment is to measure the ratio of the optical depth profiles, $\tau_\lambda = \ln\{I_\lambda/I^0_\lambda\}$ of transitions from different ionization stages of the same chemical species. For example, one could select Si II *(16 eV) and* Si IV *(45 eV) doublets, or* C II *(24 eV) transitions and the* C IV *doublet (64 eV). If one selects transitions for which the ionization potentials are two close, then there is some lost leverage on the amount that the ratio will change. If one selects transitions for which the ionization potentials are very different, for example* O I *(13 eV) and* O VI *(138 eV), then there is some uncertainty that the two ionic species arise in the same parcel of absorbing gas. At any rate, measurements are required at two epochs. One measures the statistical significance (yes, requires knowing the uncertainties precisely) at which the optical depth profile have changed from one epoch to the next. Equivalent width ratios will also do.*

If the hypothesis is that the absorbing cloud has moved relative to the source from one epoch to the next, then the observable signature of a change in the velocity distribution of the optical depth should equally be present in multiple profiles. In this case, ambiguity is reduced if the different chemical species are examined for which the ionization levels of the transitions are nearly similar. By using similar ionization levels, one minimizes the contribution of a possible change in the source luminosity as well. For example, C II *and* Si II*, or* C IV, S IV *and* N V *(97 eV) might be useful choices. If the covering fraction changes in a statistically consistent way between transitions of similar ionization levels, this is also a supportive result.*

Of course, both processes can be occurring simultaneously, and so it would be ideal to run both experiments simultaneously. The major challenge for the experiment is spectral coverage. For limited telescope time, perhaps a one shot chance for each epoch, it may not be possible to obtain the requisite signal–to–noise ratio for multiple spectral coverage settings. Since the experiment is a difference measurement, the signal–to–noise ratio needs to be at least a factor of $\sqrt{2}$ better for each epoch than would be for single epoch measurements. Also, the atmospheric cutoff or instrument plus telescope throughput may limit the useful spectral region.

4. **[15 pts]** The Partial Covering Fraction

(a) [2 pts] Define and/or describe what partial covering is.

Partial covering refers to the geometric configuration when the observed cross sectional area of the source is not fully occulted by the absorbing material.

(b) [2 pts] Define the covering fraction, C_f.

If the occultation of the source by the absorbing material is partial, then only a fraction of the source is occulted. The covering fraction is the ratio of the solid angle of the source that is occulted to the total solid angle of the source. Equivalently, this is the fractional area of the source that is occulted by the absorbing material.

(c) [4 pts] In Figure 1 of the paper, what characteristic feature of the N V $\lambda\lambda 1238, 1242$ doublet is suggestive that this absorber shows the signs of partial covering. Be specific.

The N V $\lambda\lambda 1238, 1242$ *doublet absorption is well resolved. Both members of the doublet are saturated, which is directly apparent from the fact that the line cores are flat over a broad velocity range and that the flux level of the saturated core of the* N V $\lambda 1238$ *profile is equal to that of the* N V $\lambda 1242$ *profile. In other words, the equivalent widths of the two doublet members are equal, which is the tall tale sign of optically thick gas and saturated doublet profiles. Thus, the gas is optically thick to* N V *absorption. It is clear that the source is only partially occulted because the saturated line cores do not have zero transmitted flux (saturated absorption lines that are resolved have zero flux in their cores).*

(d) [3 pts] Briefly, qualitatively describe why this characteristic feature arises in these absorption lines– think of the light paths from the source to the observer.

The absorption arises from the gas the occults the QSO. The optical depth of this gas cloud is quite high, much greater than unity. Thus, there is effectively zero transmission of the light from the occulted portion of the QSO. Light emitted from the projected area of the QSO that is not occulted has 100% transmission. The combine effect is that saturated absorption profiles are observed from absorbing gas cloud, but the line cores are "filled in" by the unocculted light. In the line core, the ratio f_λ / f^0_λ *is called the residual flux.*

(e) [4 pts] Describe how this characteristic feature of the absorption profile would change if C_f were somewhat smaller than it is.

If the covering fraction is made smaller, then the projected area of the QSO occulted by the absorbing gas is reduced. The net result is that a greater proportion of the light from the source has 100% transmission to the observer. Thus, as the covering fraction is reduced, the amount of light available to "fill in" the line cores increases. Or, as the covering fraction is decreased, the residual flux level in the line cores increases (they are shallower).

5. **[25 pts]** Consider the geometric configuration in the included diagram (Figure 1). Show that the observed flux, f_λ, is given by

$$f_\lambda = f^0_\lambda \left[1 + C_f\left(\exp\{-\tau_\lambda\} - 1\right)\right],$$

where τ_λ is the optical depth of the absorbing cloud, and where

$$f^0_\lambda = \pi \frac{R_s^2}{D^2} I^0_\lambda \quad \text{and} \quad C_f = \sin^2\theta_\lambda.$$

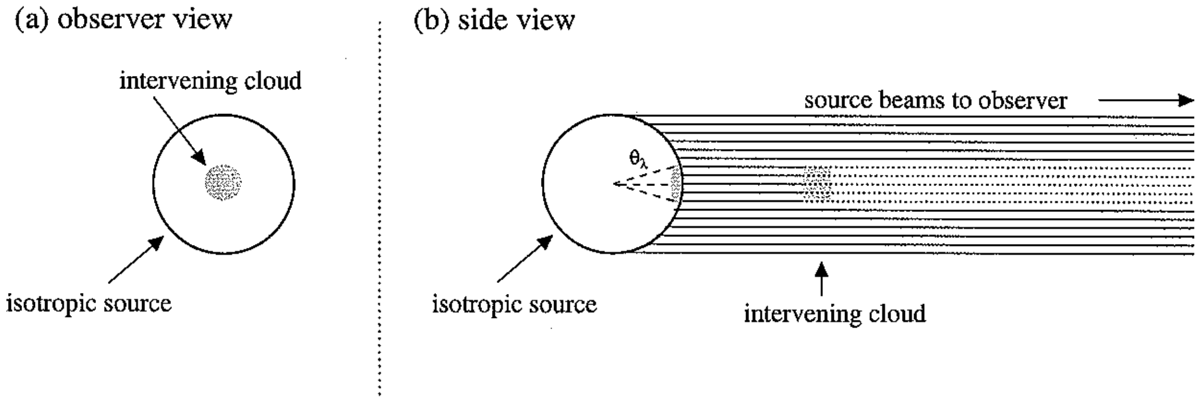

Figure 1: — A schematic of partial covering for a highly idealized case in which an absorbing cloud is centered directly in front of the disk of the source. The observed solid angle of the absorbing cloud (darker shading) is smaller than the observed solid angle of the source. In this scenario, the intervening cloud occults a area on the source (lightly shaded) defined by a cone with angle θ_λ. Solid lines from the isotropically emitting source are specific intensity beams that are unobstructed by the intervening absorber, whereas dotted lines are beams for which some level of absorption has occurred.

Start with the flux integral over the source (QSO)

$$f_\lambda = \int_\phi \int_\theta I_\lambda \cos\theta \, d\Omega,$$

where I_λ is the observed specific intensity, and $d\Omega$ is the solid angle element on the surface of the source of radius R_s as seen from the observer at a distance D. Use the fact that $I_\lambda = I^0_\lambda \exp\{-\tau_\lambda\}$ for the light beams transmitted through the absorber, where I^0_λ is the specific intensity (isotropic) emitted at the surface of the source. Show each of the following steps.

(a) [4 pts] What is the expression for $d\Omega$?

The problem stated that $d\Omega$ is the solid angle element on the surface of the source of radius R_s as seen from the observer at a distance D. The general definition of the solid angle element is $d\Omega = dA/D^2$, where dA is the line of sight projected area element as seen from the observer a distance D from the area element. On the surface of a spherical object of radius R_s, the area element is $dA = R_s^2 \sin\theta \, d\theta \, d\phi$. As viewed from the observer, we then have $d\Omega = (R_s^2/D^2)\sin\theta \, d\theta \, d\phi$. A common mistake here, was that most students provided the solid angle as seen from the center of the source, which is $d\Omega = (R_s^2/R_s^2)\sin\theta \, d\theta \, d\phi = \sin\theta \, d\theta \, d\phi$, which was incorrect.

(b) [5 pts] What are the limits of integration over the source?

From the question, which states, "start with the flux integral over the source", and from part (b) of the question, which asks for the limits of integration "over the source", you hopefully deduced that the flux is determined by integrating over the geometry of the source. That is, the origin of the coordinate system is the source center, not the position of the observer. The $\cos\theta$ factor in the flux integral is the dot product of the angle between the radial direction of the light beams emitted at the surface of the source and the direction to the observer, i.e., $\hat{\mathbf{r}} \cdot \hat{\mathbf{s}}$, where the observer is in the $\hat{\mathbf{s}}$ direction (the line of sight). The azimuthal angle, ϕ, rotates the area element about the $\hat{\mathbf{s}}$ axis, and varies from $0 \leq \phi \leq 2\pi$. The polar angle, θ can in principle range vary from $0 \to \pi$, where $\theta = 0$ is in the direction toward the *observer and $\theta = \pi$ is directly away from the observer and the angle increases counterclockwise in the diagram. However, only beams originating from the hemisphere on the observer side of the source reach the observer, so the polar angle limits of integration range from $0 \leq \theta \leq \pi/2$. (For $0 \leq \theta \leq \pi$, the flux integral vanishes!)*

(c) [6 pts] Fully write out the integrals to obtain f_λ.

As an example for illustration purposes of this solution set, we first set up the problem for no occulting cloud and then for a fully occulting cloud. The observed flux from an unocculted, unresolved spherical source of radius R_s at a distance D from the observer is

$$f^0_\lambda = \frac{R_s^2}{D^2} \int_0^{2\pi} \int_0^{\pi/2} I^0_\lambda \cos\theta \sin\theta \, d\theta \, d\phi = \pi \frac{R_s^2}{D^2} I^0_\lambda.$$

The observed flux from a fully occulted unresolved spherical source of radius R_s at a distance D from the observer is

$$f_\lambda = \frac{R_s^2}{D^2} \int_0^{2\pi} \int_0^{\pi/2} I^0_\lambda \exp\{-\tau_\lambda\} \cos\theta \sin\theta \, d\theta \, d\phi = \pi \frac{R_s^2}{D^2} I^0_\lambda \exp\{-\tau_\lambda\} = f^0_\lambda \exp\{-\tau_\lambda\},$$

where τ_λ is the optical depth of the occulting cloud. The problem here is to treat a partially occulted source as configured in Figure 1. The occulted region of the source is the surface of rotation (about ϕ) over the range of polar angle $0 \leq \theta \leq \theta_\lambda$, and the unocculted region is the surface of rotation over the range of polar angle $\theta_\lambda \leq \theta \leq \pi/2$. Writing $f_\lambda = f^{occ}_\lambda + f^{unocc}_\lambda$, we have

$$f^{occ}_\lambda = \frac{R_s^2}{D^2} \int_0^{2\pi} \int_0^{\theta_\lambda} I^0_\lambda \exp\{-\tau_\lambda\} \cos\theta \sin\theta \, d\theta \, d\phi = \sin^2\theta_\lambda \, \pi \frac{R_s^2}{D^2} I^0_\lambda \exp\{-\tau_\lambda\},$$

$$f^{unocc}_\lambda = \frac{R_s^2}{D^2} \int_0^{2\pi} \int_{\theta_\lambda}^{\pi/2} I^0_\lambda \cos\theta \sin\theta \, d\theta \, d\phi = [1 - \sin^2\theta_\lambda] \pi \frac{R_s^2}{D^2} I^0_\lambda.$$

(d) [5 pts] Integrate (Hint: try the substitution $\mu = \cos\theta$).

We wish to show the evaluation of the above integrals (this section is for purpose of illustration of this solution set, it was not required that this substition be shown, since there are multiple ways to solve the integral). Clearly the integral over the azimuthal angle is simply 2π, the factor for the surface of rotation. For the polar angle, if we use $\mu = \cos\theta$, then $d\mu = -\sin\theta d\theta$. The integrand simplifies to $-\mu \, d\mu$. The limits of integration transpose to $(\theta = 0 \to \mu = 1)$, $(\theta = \pi/2 \to \mu = 0)$, and $(\theta = \theta_\lambda \to \mu = \cos\theta_\lambda)$. We thus have

$$f^{occ}_\lambda \propto - \int_1^{\cos\theta_\lambda} \mu \, d\mu = -\frac{1}{2}\mu^2 \Big|_1^{\cos\theta_\lambda} = \frac{1}{2}(1 - \cos^2\theta_\lambda) = \frac{1}{2}\sin^2\theta_\lambda,$$

$$f^{unocc}_\lambda \propto - \int_{\cos\theta_\lambda}^{0} \mu \, d\mu = -\frac{1}{2}\mu^2 \Big|_{\cos\theta_\lambda}^{0} = \frac{1}{2}\cos^2\theta_\lambda = \frac{1}{2}[1 - \sin^2\theta_\lambda].$$

Thus, we have the factors $\sin^2\theta_\lambda$ and $[1 - \sin^2\theta_\lambda]$ for f^{occ}_λ and f^{unocc}_λ, respectively.

(e) [5 pts] Algebraic manipulation to obtain the final result.

Writing $f_\lambda = f^{occ}_\lambda + f^{unocc}_\lambda$, we have

$$f_\lambda = \sin^2\theta_\lambda \, \pi \frac{R_s^2}{D^2} I^0_\lambda \exp\{-\tau_\lambda\} + [1 - \sin^2\theta_\lambda] \pi \frac{R_s^2}{D^2} I^0_\lambda,$$

Setting $C_f = \sin^2\theta_\lambda$ and invoking $f^0_\lambda = \pi(R_s^2/D^2) I^0_\lambda$, yields

$$f_\lambda = C_f f^0_\lambda \exp\{-\tau_\lambda\} + [1 - C_f] f^0_\lambda,$$

where the first term on the right hand side is the flux that is transmitted through (survives not being absorbed in) the occulting cloud, and the second term is the unocculted flux that passes directly to the observer. Simple steps yield the desired form quoted above.

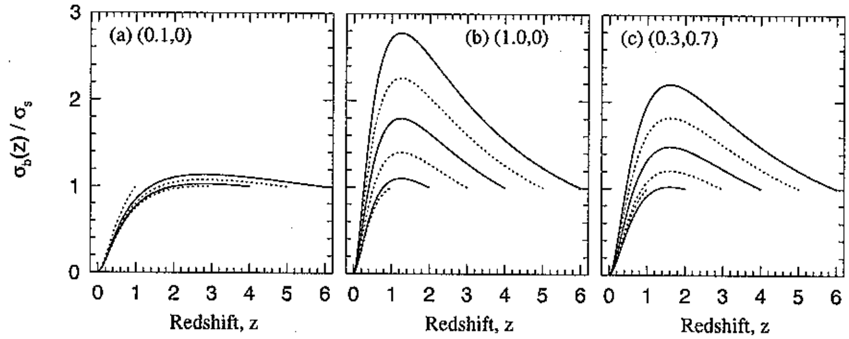

Figure 2.15: The redshift dependence of the cross section of a beam, $\sigma_b(z)$ for sources with cross section σ_s at redshift z_s, given by Eq. 2.157. Six source redshifts are illustrated, $z_s = 1$, 2, 3, 4, 5, and 6. Solid curves represent even z_s and dotted curves represent odd numbered z_s. — (a) the low–density cosmology (0.1,0). — (b) the Einstein–de Sitter (1.0,0) cosmology. — (c) the Λ cosmology (0.3,0.7).

explains the difference
-tween recessional
and peculiar velocities
- you needed to apply
peculiar velocities
for #2 on the Curve
check out Eq 2.171

2.8 Velocity and Redshift

Having defined the connections between redshift and time and also various distances, it is of interest to consider the concept of velocity, which is derived from the ratio of proper distance over travel time. The proper distance is

$$l = \frac{a(t)}{a_0} D_c = \frac{D_c}{1+z}, \tag{2.158}$$

where the co–moving distance is given by Eq. 2.113. Velocity is the time derivative of the proper distance,

$$v = \frac{dl}{dt} = \frac{\dot{a}(t)}{a_0} D_c + \frac{a(t)}{a_0} \dot{D}_c. \tag{2.159}$$

Writing $v = v_{\rm rec} + v_{\rm pec}$, we have the definitions of the cosmological velocity of recession (due to Hubble flow) and the so–called peculiar velocity,

$$v_{\rm rec} = \frac{\dot{a}(t)}{a_0} D_c \qquad v_{\rm pec} = \frac{a(t)}{a_0} \dot{D}_c. \tag{2.160}$$

The deduced (not observed) velocity of recession is dependent upon the expansion velocity at the epoch of the observation, $\dot{a}(t)$, where the observer is not necessarily in the inertial frame of the object, as will discussed in § 2.8.3. The peculiar velocity of an object, on the other hand, measures an objects velocity difference with respect to the Hubble flow. It can also be applied to determine the velocity difference between two cosmological objects assumed to be undergoing identical Hubble flow.

2.8.1 Peculiar Velocities

The peculiar velocity is defined in the inertial frame of the object. Thus, the observer must apply a transform (rigorously or assumed) to place a cosmological object in its inertial frame. As such, peculiar velocities obey the rules of special relativity. As will be discussed below, measurement of the redshift of a cosmological object directly yields the co-moving peculiar velocity, $\dot{D}_c$. To obtain the inertial–frame peculiar velocity, $v_{\rm pec}$ (or what is commonly called the rest–frame peculiar velocity), $\dot{D}_c$ is multiplied by the ratio $a(t)/a_0$. No object can have a peculiar velocity exceeding light speed.

difference of effect

2.8.1.1 Photons

The peculiar velocity of a photon is always the speed of light, c. Photon velocities can be derived from the definition of $v_{\rm pec}$ and the fact that photons travel on geodesics, $ds = 0$. Rewriting $\dot{D}_c = dD_c/dt$, and applying the chain rule, photons have

$$v_{\rm pec} = \frac{a(t)}{a_0}\frac{dD_c}{dt} = \frac{a(t)}{a_0}\frac{dD_c}{d\chi}\frac{d\chi}{da}\frac{da}{dt} = c, \tag{2.161}$$

which is obtained by substitution of Eqs. 2.51, 2.54, and 2.52 (rearranged), respectively,

$$\frac{dD_c}{d\chi} = \frac{D_{\rm H}}{\sqrt{\Omega_k}}, \qquad \frac{d\chi}{da} = \frac{a_0}{a^2(t)}\frac{\sqrt{\Omega_k}}{E(t)}, \qquad \frac{da}{dt} = c\,\frac{a(t)E(t)}{D_{\rm H}}, \tag{2.162}$$

into Eq.2.161. Application of the geodesic, i.e., $ds = 0$, is applied through the co–moving coordinate, $d\chi/da$, since this relationship in particular is derived for photons only.

2.8.1.2 Cosmological Objects

The peculiar velocity of an object is defined as its velocity relative to the local cosmological velocity of recession, i.e., relative to the Hubble flow. Peculiar velocities are induced by mechanical and dynamical interactions. As observers, we can measure only the radial (line of sight) component of the peculiar velocity via the *observed* redshift of the source object, z_s, which is almost always obtained by a spectroscopic measurement of a redshifted absorption or emission line at wavelength λ_o for which the rest–frame wavelength is known to be λ_r.

Consider an inertial reference frame at cosmological redshift z, in which a source object is observed to have redshift z_s. The line of sight component of the peculiar velocity induces a small observed redshift offset, $\Delta z = z_s - z$, relative to the local cosmological redshift. From the measured Δz, and assuming $v_{\rm pec} \ll c$, the peculiar velocity is

$$\dot{D}_c = c\,\Delta z \quad \text{or} \quad v_{\rm pec} = \frac{c\,\Delta z}{1+z}, \tag{2.163}$$

where $v_{\rm pec} = [a(t)/a_0]\dot{D}_c = \dot{D}_c/(1+z)$ follows from Eq. 2.160. The expression for $v_{\rm pec}$ can also be obtained directly from the non–relativistic Doppler formula,

$\Delta v/c = \Delta\lambda/\lambda$. If $\lambda_o = \lambda_r(1+z_s)$ is the observed wavelength and λ_r is the rest–frame wavelength for an emitter or absorber at redshift z, then

$$\frac{v_{\rm pec}}{c} = \frac{\Delta v}{c} = \frac{\Delta\lambda}{\lambda} = \frac{\lambda_r(1+z_s)-\lambda_r(1+z)}{\lambda_r(1+z)} = \frac{(1+z_s)-(1+z)}{(1+z)}, \qquad (2.164)$$

non-relativistic

where the observed wavelength can be expressed in terms of the redshift offset, $\lambda_o = \lambda_r(1+z_s) = \lambda_r(1+z+\Delta z)$, yielding

$$\frac{v_{\rm pec}}{c} = \frac{\Delta\lambda}{\lambda} = \frac{(1+z+\Delta z)-(1+z)}{(1+z)} = \frac{\Delta z}{1+z}. \qquad (2.165)$$

Relaxing $v_{\rm pec} \ll c$, we are required to employ the well known relativistic Doppler formula to obtain the peculiar velocity,

$$1+\Delta z = \sqrt{\frac{1+\dot{D}_c/c}{1-\dot{D}_c/c}} \quad \text{or} \quad 1+\frac{\Delta z}{1+z} = \sqrt{\frac{1+v_{\rm pec}/c}{1-v_{\rm pec}/c}}, \qquad (2.166)$$

relativistic

where the factor $1+z$ ensures that $v_{\rm pec}$ is the inertial frame peculiar velocity (omitting the normalization provides the co–moving peculiar velocity $\dot{D}_c$). Inverting, we have

$$v_{\rm pec} = c\,\frac{\left[1+\dfrac{\Delta z}{1+z}\right]^2 - 1}{\left[1+\dfrac{\Delta z}{1+z}\right]^2 + 1}, \qquad (2.167)$$

which reduces to Eq. 2.163 for $\Delta z/(1+z) \ll 1$.

2.8.2 Observed and Inertial–Frame Velocity Separations

The peculiar velocity, $v_{\rm pec} = [a(t)/a_0]\dot{D}_c$, can also be applied to obtain the line of sight velocity separation between two cosmological objects. However, it must be assumed that the two objects reside in the same inertial frame (share the same time coordinate). The term $\dot{D}_c$ is interpreted as the co–moving peculiar velocity. As we shall see, when a redshift offset, Δz, is measured between two cosmological objects, this is a direct measurement of $\Delta\dot{D}_c$; thus, the co–moving velocity separation is actually the line of sight velocity separation in the observer frame (a trivial statement). To convert to the object "rest frame", one must correct the observer frame velocity separation by the expansion factor of the local frame, $a(t)/a_0 = (1+z)^{-1}$.

Consider two cosmological objects along the same line of sight such that object 1 has observed redshift z_1 and object 2 has observed redshift z_2. If $z_1 \neq z_2$, the two objects have a non–zero velocity relative to one another. Assuming the redshift offset is due to peculiar velocities, in the case that $z_1 \simeq z_2$, the inertial frame velocity separation between the objects along the line of sight is

$$\Delta\dot{D}_c = c\,\Delta z \quad \text{or} \quad \boxed{\Delta v = \frac{c\,\Delta z}{1+\bar{z}}} \qquad (2.168)$$

this one

or

$\Delta z = z_1 - z_2$

$\bar{z} = \frac{1}{2}(z_1+z_2)$

or z_2

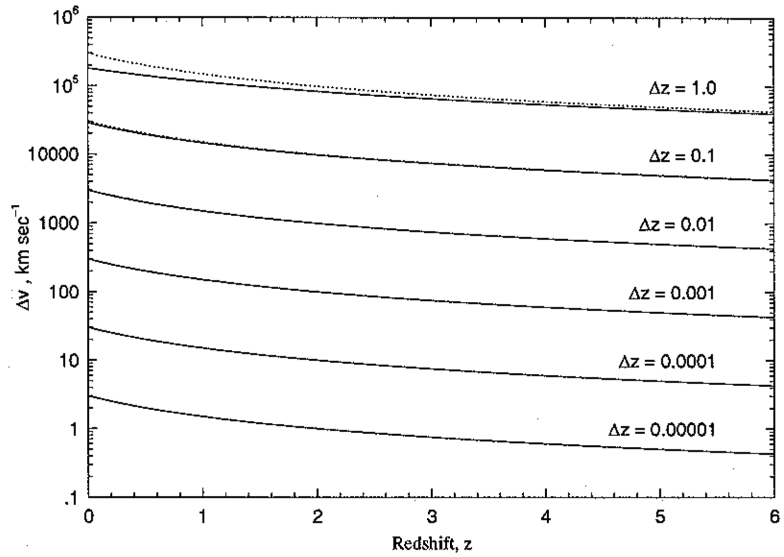

Figure 2.16: — The rest–frame velocity separation, Δv, between two cosmological objects at redshift z with redshift offsets of $\Delta z = 0.00001$, 0.0001, 0.001, 0.01, 0.1, and 1.0. The solid curves are given by Eq. 2.170, the full relativistic formula, and the dotted curves are given by Eq. 2.168, for non–relativistic velocities. Note that the non–relativistic treatment is a good approximation for $\Delta z \leq 0.1$. Thus, the rule of thumb (Eq. 2.169), which shows how Δv scales with Δz anchored at $\Delta z = 0.0001$ yielding $\Delta v = 30/(1+z)$ [km sec^{-1}], can be applied for a large range of Δz.

where $\Delta z = z_1 - z_2$, and $\bar{z} = (z_1 + z_2)/2$. Eq. 2.168 follows from the same principles applied to obtain Eq. 2.163. A good rule of thumb is $\Delta z = 0.0001$ yields $\Delta \dot{D}_c = 30$ [km sec^{-1}] for the line of sight velocity separation in the observer frame. The inertial frame line of sight velocity separation is computed by dividing by $1 + \bar{z}$,

this one

$$\boxed{\Delta v = \frac{\Delta z}{0.0001} \cdot \frac{30}{1+\bar{z}} \ \text{km sec}^{-1}.} \qquad (2.169)$$

Here, the speed of light has been rounded to 3.0×10^5 [km sec^{-1}]. For example, for $\Delta z = 0.002$ at $\bar{z} = 1$, the inertial frame velocity separation is approximately $\Delta v = 20 \cdot (30/2) = 300$ [km sec^{-1}],

or

this formula would have been correct for #2 on the curve

For a redshift offset of $\Delta z = 0.1$, Eqs. 2.168 and 2.169 overpredict Δv by 5%. The relativistic expression for inertial frame velocity separation of object 1 relative to object 2 is

$$* \qquad \boxed{\Delta v_{12} = c\,\frac{(1+z_1)^2 - (1+z_2)^2}{(1+z_1)^2 + (1+z_2)^2},} \qquad (2.170)$$

as derived directly from Eq. 2.167 for $\Delta z = z_1 - z_2$ and $z = z_2$. If $z_1 < z_2$, then Δv_{12} is negative, which is to be interpreted such that the object 1 is moving toward the observer relative to object 2. The derivation of Eq. 2.170 for the velocity separation of object 2 relative to object 1 yields a simple switching of subscripts on the redshifts, which yields $\Delta v_{21} = -\Delta v_{12}$. It is straight forward to show that Eq. 2.170 reduces to Eqs. 2.168 and 2.169 in the limit $z_1 \simeq z_2$.

Eqs. 2.170 (solid curves) and 2.168 (dotted curves) are illustrated in Figure 2.16 for various redshift offsets as a function of redshift. Note that the curves obey Eq. 2.169 for a large range of Δz; it is not until $\Delta z = 0.1$ that the relativistic treatment becomes necessary.

2.8.3 Velocities of Recession

most of you used this formula!!

Applying the relativistic formula (Eq. 2.170) for large redshift objects, as observers at $z = 0$, we would naively assign an apparent recession velocity of

$$v_{\rm rec} = c\,\frac{(1+z)^2 - 1}{(1+z)^2 + 1} \qquad \text{(incorrect)} \tag{2.171}$$

never ever!

to a cosmological object at redshift z. Wrong; don't ever do this. It should remain appreciated that the cosmological velocity of recession is <u>not</u> an inertial frame measurement and thus does not obey the rules of special relativity. To apply Eq. 2.171 as a means of determining a velocity of recession to a cosmological object is flat out incorrect.

* Recession velocities are not interpreted as a Doppler shift. Yet, a consequence of the expanding universe paradigm is that redshift is directly related to recessional velocity (Harrison, 1993). There has been great confusion over the interpretation of this velocity because of the notion that no objects can recede at faster than light speed. Actually, it is an intellectual misconception that the velocities of objects carried by the Hubble flow cannot exceed the speed of light (see Davis & Lineweaver, 2004). In the expanding universe formalism, there is no global reference frame. It is general relativity and not special relativity that is employed for computing cosmological dynamics.

In general relativity, motions outside the observer's inertial reference frame can be properly treated and can be fully consistent with faster than light speed motion. From Eq. 2.160, we have

$$v_{\rm rec} = \frac{\dot{a}(t)}{a_0} D_c, \tag{2.172}$$

where, in general, $t = t_o$ is the cosmological time of the observation (for a present epoch observer, $t_o = t_0$). Rearranging $\dot{a}(t_o)/a_0$ gives

$$\frac{\dot{a}(t_o)}{a_0} = \frac{\dot{a}(t_o)}{a(t_o)}\frac{a(t_o)}{a_0} = \frac{H(z_o)}{1+z_o} = \frac{H_0 E(z_o)}{1+z_o}, \; * \tag{2.173}$$

where z_o is the redshift of the observer, and where $E(z_o)$ is given by Eq. 2.81. Eq. 2.173 can be interpreted as a "proper expansion rate" of the universe for an observer at redshift z_o (as will be further discussed below). The co-moving distance appearing in Eq. 2.172 is the co-moving radial separation, $D_c(z_o, z_s)$,

$$* \; E(z) = \frac{H(z)}{H_0} = \left\{ \Omega_m (1+z)^3 + \Omega_\Lambda \right\}^{1/2}$$

between the observer and the source (see § 2.7.2). From Eq. 2.117, and noting that $c = H_0 D_{\rm H}$, the velocity of recession is then

$$v_{\rm rec}(z_o, z_s) = \frac{c\,E(z_o)}{1+z_o}\int_0^{z_{os}} \frac{dz}{E(z)} = \frac{c\,E(z_o)}{1+z_o}\frac{D_c(z_o,z_s)}{D_{\rm H}}, \qquad (2.174)$$

where z_{os} is the reduced redshift (Eq.2.116),

$$1 + z_{os} = \frac{1+z_s}{1+z_o}, \qquad (2.175)$$

for an observed source redshift, z_s.

2.8.3.1 Present Epoch Observer

For present epoch observers, $z_o = 0$, so that the factor $E(z_o)/(1+z_o)$, is unity. The co–moving radial separation reduces to the total co–moving distance (Eq. 2.113). Thus, Eq. 2.174 simplifies to

$$v_{\rm rec}(0,z) = c\int_0^{z} \frac{dz}{E(z)} = c\,\frac{D_c}{D_{\rm H}}. \qquad (2.176)$$

how you compute cosmological velocity of recession! see Fig 2.17

The recessional velocity of cosmological objects for a present epoch observer is simply a multiple of the the speed of light, where that multiple is the number of Hubble distances to the object. For $D_c/D_{\rm H} < 1$, $v_{\rm rec}(0,z)$ is some fraction of light speed. For $D_c/D_{\rm H} > 1$, $v_{\rm rec}(0,z)$ is greater than the speed of light. When the co–moving distance is the Hubble distance, $v_{\rm rec}(0,z) = c$.

In Figure 2.17, the recession velocity of cosmological objects is shown as a function of redshift for present epoch observers, i.e., $z_o = 0$. The low–density (dotted curve), Einstein–de Sitter (dashed), and Λ cosmologies (solid) are illustrated, as are the special relativity velocity law (Eq. 2.171) and the linear velocity law, $v = cz$.

For $z < 0.1$, the various recession velocities are consistent. For the "737" cosmology, the recession velocity exceeds the speed of light at $z \simeq 1.46$. It is important to recognize that recessional velocity is not an observed quantity; redshift is the observed quantity. Recessional velocity is a deduced quantity that has an interpretation only through the cosmological paradigm.

2.8.3.2 Observer at Arbitrary Redshift

An additional predictive power of Eq. 2.174 is that the recessional velocity for observers at different cosmic times, i.e., redshifts of observation, z_o, can be deduced (thus, Eq. 2.174 can be employed to compute the recessional velocity of a higher redshift object from the perspective of a lower redshift object). Effectively, the recessional velocity is the number of radial co–moving separations per Hubble distance, $D(z_o, z_s)/D_{\rm H}$, multiplied by the factor, $c\,E(z_o)/(1+z_o)$, which is evaluated at the redshift of observation. This factor accounts for the fact that observers at different epochs measure different cosmological expansion *rates.*

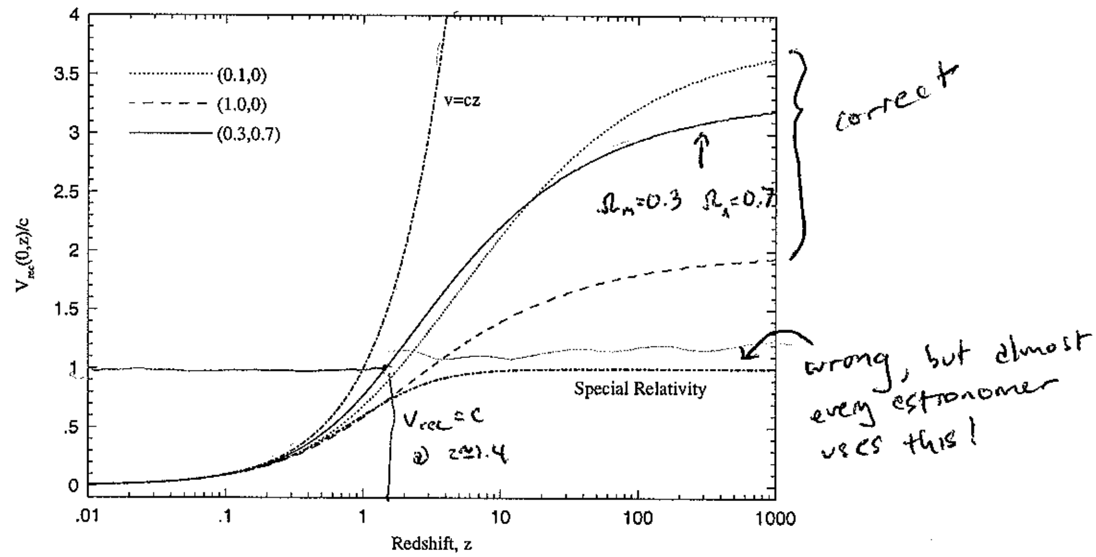

Figure 2.17: — The velocity of recession, $v_{\rm rec}(0, z)$, of objects carried by the Hubble flow as a function of redshift for a present epoch observer. Three cosmologies are shown, denoted by $(\Omega_m, \Omega_\Lambda)$; (i) the low–density (0.1,0), dotted; (ii) Einstein–de Sitter (1.0,0), dashed; and the Λ cosmology (0.3,0.7), solid. The special relativity case (Eq. 2.171) and the linear relation, $v = cz$, are shown as thick dash–dot curves. For the Λ cosmology, the recession velocity of objects exceeds the speed of light at $z \simeq 1.46$ (Figure adapted from Davis & Lineweaver, 2004)

In Figure 2.18a, the velocity of recession of cosmological sources is shown for observers at redshifts between $0 \leq z_o \leq 5.6$ in steps of 0.2 for source redshifts over the range $z_o \leq z_s \leq 50$. Each curve is for a different observer redshift, which can be identified by $v_{\rm rec}(z_o, z_s)/c = 0$ at $z = z_o$. These velocity curves can be compared to the co–moving radial separations illustrated in Figure 2.8b. Effectively, the recession velocities are those curves multiplied by factor $c\,E(z_o)/(1+z_o)$. As alluded to above, the expression $H_0E(z_o)/(1+z_o)$, given by Eq. 2.173, can be interpreted as the proper cosmological expansion rate for an observer at redshift z_o. Thus, the ratio $E(z_o)/(1+z_o)$ can be interpreted as the "normalized proper expansion rate", i.e., normalized to the expansion rate at the present epoch.

The normalized proper expansion rate for an observer at z_o is plotted in the inset of Figure 2.18a over the range $0 \leq z \leq 5$. The rate has a minimum given by Eq. 2.86 (a result that can be obtained via standard calculus) at $z = 0.7456$ and returns to unity at $z = 2.4380$.[7] For large z, the rate develops an asymptotic behavior of $\Omega_m(1+z)^{1/2}$.

The overall behavior from high to low redshift is that the proper expansion *rate* for observers decreases with decreasing redshift (deceleration) until $z \simeq$

[7]These values correspond to the current best cosmological parameters listed in Table 2.1. The curve plotted in Figure 2.18a (inset) is for the 737 cosmology parameters, which has a minimum at $z = 0.6711$ and a recover to unity at $z = 2.0888$. For the remainder of the discussion, we assume the current best values.